Asian Journal of Chemistry; Vol. 31, No. 2 (2019), 453-459

ASIAN JOURNAL OF CHEMISTRY

https://doi.org/10.14233/ajchem.2019.21696

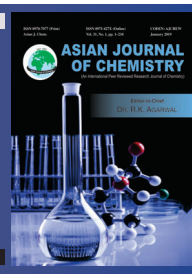

Structural, Morphological, Optical and Photoluminescence Properties of Hafnium Oxide Nanoparticles Synthesized by Sol-Gel Method

N. MAHENDRAN, S. JOHNSON JEYAKUMAR*, M. JOTHIBAS and A. MUTHUVEL

PG & Research Department of Physics, T.B.M.L. College, Porayar-609307, India

*Corresponding author: E-mail: drsjohnson@rediffmail.com

Received: 5 September 2018; *Accepted*: 3 November 2018; *Published online*: 31 December 2018; AJC-19226

The novel HfO_2 nanoparticles have been synthesized using sol-gel method. The samples were characterized by X-ray powder diffraction, scanning electron microscopy with elemental analysis, Fourier transform infrared spectrometer, UV-visible spectroscopy. The XRD patterns revealed the transition of cubic to monoclinic phase and calculated particle sizes are 34.92 and 35.66 nm in cubic phase and increase in molar concentration increased the size to 60.31 and 60.33 nm. The optical band gap energy decrease with increasing molar concentrations. We expect that this sol-gel method may be extended to the preparation of nanostructures of other kinds of metal oxides.

Keywords: Hafnium oxide, Nanoparticles, Sol-gel, Photoluminescence.

INTRODUCTION

Nanostructured materials have a lot of important applications in various fields because of their unique properties. Semiconductor nanoparticles have received much attention because of their special properties in comparison with those of bulk materials [1-3]. In particular, inorganic compound hafnium oxide (HfO_2) is an important group II-IV semiconductor with a wide band gap (5.7eV) [4]. Hafnium dioxide is a material with a number of technologically attractive properties such as high melting point (2758 °C), high dielectric constant (≈ 30), high chemical stability and high neutron absorption cross section [5]. It often plays an important role in the continuous down-scaling of integrated circuits since new insulating materials with a high dielectric constant are being researched to replace SiO_2 as a gate dielectric. In terms of structural characteristics, hafnium oxide exists in three polymorphic structures, namely monoclinic (m-HfO_2) at low temperature, tetragonal (t-HfO_2) above 2050 K and cubic (c-HfO_2) at around 2803 K. Each structure has different applications. In past years researchers have been fascinated with nanoparticles structure. Materials with their enormous potentials found in different ways of uses for example semiconductor, optics, magnetic data storage, catalysis ceramics and nano composites. Hafnium oxide has high refractive index and laser damage thresholds [6]. In previous years many ways prepared nanoparticles like, cobalt, platinum, germanium and gold have been embedded into the hafnium oxide matrix to develop the interfacial and electrical properties of semiconductor-metal-oxide devices [7].

Many different ways have been reported for the produced metal oxides nanoparticles. We designed an experiment to synthesize europium doped HfO_2 nanoparticles, using a sol-gel method. In the sol-gel method, the chemical reaction is comparatively simple, low-cost and non-toxic compared to other synthetic methods includes solvothermal [8], hydrothermal [9], non-hydrolytic synthesis [10]. The techniques of precipitation method has many advantages, including low cost and good composition process [11]. The possibility of using HfO_2 as a high –k-dielectric [12] in capacitor devices in memory board such that dynamic random access memory (DRAM) applications stimulated a scientific and technique interest in it [13]. The obtained HfO_2 NPs were characterized by X-ray diffraction (XRD) and Fourier transform infrared (FTIR) spectroscopy. The optical properties were studied by UV and photoluminescence. The morphology and size of the HfO_2 NPs were evaluated by scanning electron microscope (SEM).

EXPERIMENTAL

Hafnium chloride (purity 98 %) was purchased from Alfa Aesar South Korea. Sodium hydroxide was procured from spectrum in India. All the above mentioned chemicals are of Research grade that can be used without futher purification.

Synthesis of hafnium dioxide (HfO_2) nanoparticles: The synthesis of HfO_2 NPs were by sol-gel method using hafnium tetrachloride ($HfCl_4$) and NaOH was added slowly into a NaOH 0.2, 0.4, 0.6 and 0.8 M aqueous solution of $HfCl_4$ and allowed to vigorous stirring using for 3 h. Finally white coloured precipitate was containing hafnium hydroxide was obtained. The $Hf(OH)_4$ precipitated was washed thoroughly with distilled water and centrifuged at 3000 rmp for 20 min to remove the residuals. The process was repeated several times until the precipitate was free from any trace of impurities. The obtained $Hf(OH)_4$ precipitate was dried in an air hot oven at 100 °C for 1 h and further calcined at 500 °C for 2 h resulting in the formation of hafnium dioxide (HfO_2) nanoparticles.

Characterization of the samples: Structural analysis was carried out using X-ray diffractometry using CuK_α radiation (λ = 1.5406 Å) operated at 40 kV and 30 mA in the wide angle region of 2θ range from 30° to 70°. Morphology and microstructure were identified by scanning electron microscope (SEM Philip XL 30). Formation of HfO_2 in wurtzite phase and available molecular bonds were investigated by the FTIR absorption spectrum. To investigate the optical properties of these nanoparticles, the absorbance spectra of the samples were obtained using UV-visible spectrometer (model: Lambda 35, make Perkin) in the wave length range 300 to 1000 nm using quartz cuvettes at room temperature. The photoluminescence (PL) spectrum of the HfO_2 nanoparticles dissolved in methanol has been measured using a spectrophotometer in the range of 4000 to 400 cm^{-1}, (F-2500 FL Spectrophotometer, Hitachi).The electrical conductivity study is carried out by using (Keithley 2636 B source meter).

RESULTS AND DISCUSSION

Structural studies: The crystal structure of hafnium oxide nanoparticles sample with different molar concentrations are shown in Fig. 1. The peak positions are in good agreement with the standard HfO_2 (JCPDS: 53-0560). The XRD spectra of powder sample calcinated at0.05M have four well resolved peaks at 2θ = 30.3°, 35.2°, 50.5°, 60.2° and 74.8°, which are indexed as reflection from (111), (002), (002) and (113) planes, respectively and these peaks are indexed corresponding to the cubic phase of HfO_2 NPs. However the molarity increased from 0.1 M, the intensity of the peak also increased, due to improvement of cubic crystal nature. At the molarities (0.15-0.2 M) six well resolved peaks at 2θ = 31.6°, 34.1°, 35.8°, 41.0°, 45.4° and 50.4° which indexed as reflection from (011), (111), (002), (112), (220) and (113) planes are observed respectively. These indexed peaks are correspond to pure monoclinic phase HfO_2which was observed and also well matched with sterdeged pattern (JCPDS No. 78-0049).

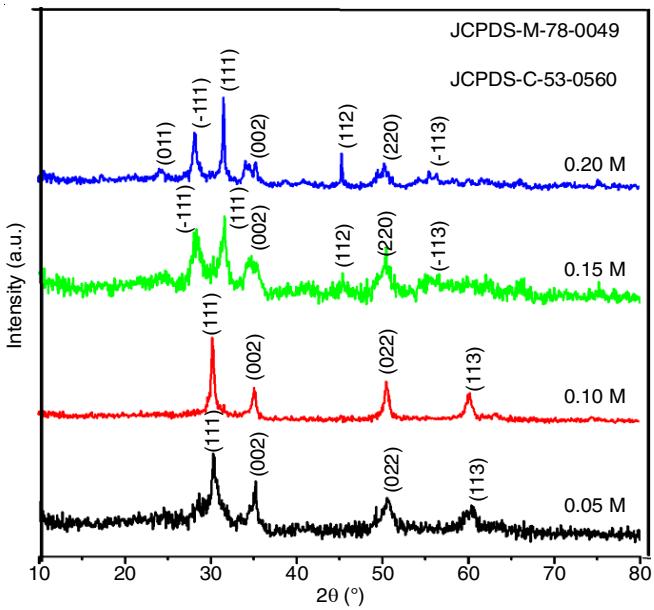

Fig. 1. XRD patterns of hafnium oxide (HfO_2) nanoparticles for various molarity concentrations

The crystallite size has been inferred from 2θ and the full width at half maximum (FWHM) of (111) diffraction peaks on the basis of the Scherrer's relation:

$$D = \frac{K\lambda}{\beta\cos\theta} \quad (1)$$

where D is the average crystallite size (Å), K is the shape factor (0.9), λ is the wavelength of X-ray (1.5406 Å) at CuK_α radiation, θ is the Bragg angle and β is the corrected the line broadening of the nanoparticles [14].

The calculated crystal size increases with increase of molarity (0.05-0.1 M) and then double time increase in crystal size for higher molarity (0.15-0.2 M). It means that the increase showed at higher molar concentration observed with decrease in FWHM of the peak It is also evident from Table-1.

The lattice constants a = b = c were calculated using the following formula used for cubic systems [15]:

$$d = \frac{a}{\sqrt{h^2 + k^2 + l^2}} \quad (2)$$

where d is the lattice spacing, a, b and c are the lattice constants, h, k and l are the miller indices, θ is the angle of corresponding peak and λ is the wavelength of X-ray used (1.5406 Å). The

TABLE-1
STRUCTURAL PARAMETERS OF HfO_2 NANOPARTICLES

Molarity (M)	2θ (°)	Crystallite size (D) (nm)	Dislocation density (δ) × 10^{14} lines/m^2	Microstrain (ε)	Lattice constants (Å)	Crystal structure
0.05	30.32	34.97	8.177	0.0013	5.14	Cubic
0.10	30.33	35.06	8.133	0.0010	5.13	Cubic
0.15	31.63	60.31	2.744	0.0006	4.88	Monoclinic
0.20	31.65	60.33	2.746	0.0006	4.85	Monoclinic

lattice constant showed an increase with increase of molarity (0.05-0.1M), which is due to improvement of crystallinity in cubic phase. At increased higher molarities (0.1-0.2 M) the lattice crystal decreased which means the crystal transforms from cubic to monoclinic phase.

The structural parameters are calculated from the following equations [16]:

$$\text{Microstrain:} \quad \varepsilon = \frac{\beta \cos\theta}{4} \tag{3}$$

$$\text{Dislocation density:} \quad \delta = \frac{1}{D^2} \tag{4}$$

The lattice defects like microstrain and dislocation density showed a decreasing trend with increasing from molarity which may be due to the improvement of crystallinity as well as the high orientation along (111) direction (Fig. 1).

Optical study

Evaluation of band gap energy: The optical behaviour of hafnium oxide nanoparticles were studied by UV absorption spectroscopy. The UV absorption spectrum of the hafnium nanoparticles as shown in Fig. 2. The absorption edge was found at shorter wavelength in the UV region at 210 nm. The absorption co-efficient is calculated using the formula:

$$\alpha = \frac{2.303A}{l}$$

where, A is the absorbance and *l* is the path length. The value of optical band gap is determined from the absorption spectra using the Tauc relation [17],

$$\alpha h\nu = A(h\nu - E_g)^n$$

where, α is the absorption coefficient, A is the constant having separate value for different transitions, $h\nu$ is the photon energy and E_g is the band gap energy. The value of n depends upon the nature of transition. The values of n for allowed direct, allowed indirect, forbidden direct and forbidden indirect transitions are 1/2, 2, 3/2 and 3, respectively. The band gap energies are found to be a negative number for n = 2, 3/2 and 3 and hence the relationship fitting to the HfO_2 is n = 1/2, which confirms the allowed direct transition. Fig. 3 shows the curves of $(\alpha h\nu)^2$ *versus* $h\nu$ for pure HfO_2 nanoparticles prepared at different molarities. The E_g values were obtained by extrapolating the straight line portions of the graph to the X-axis. The measured energy band gaps from these plots are represented in Table-2. From this table, it can be observed that the E_g values varied from 5.9 to 6.2 eV for pure HfO_2 nanoparticles prepared at optimized temperature [18].

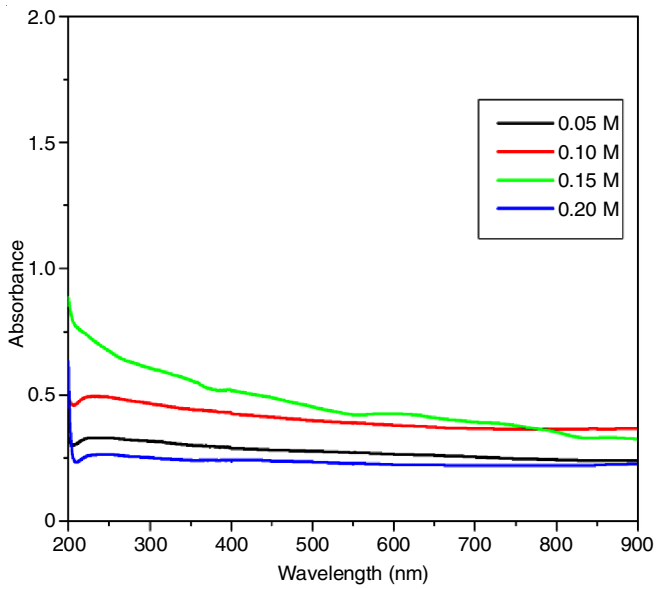

Fig. 2. Optical absorption spectra of hafnium oxide (HfO_2) nanoparticles at various molarities

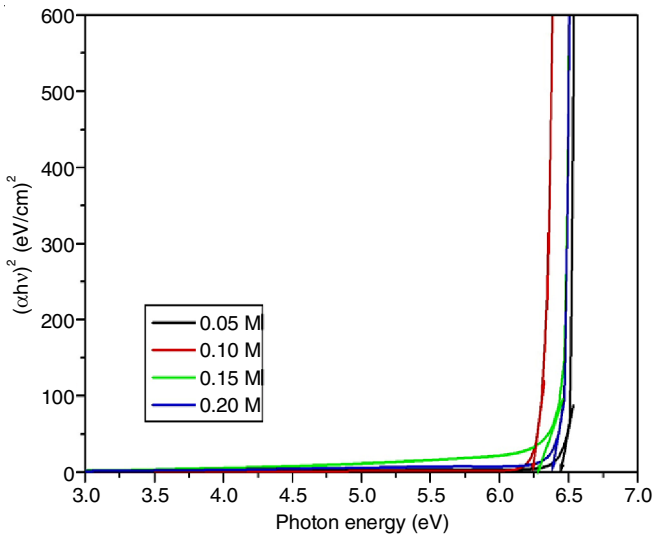

Fig. 3. Optical band gap spectra of hafnium oxide (HfO_2) nanoparticles at various molarities

TABLE-2
VARIATION OF ABSORPTION EDGES AND ENERGY BAND GAP OF HfO_2 NANOPARTICLES AT VARIOUS MOLARITY

Molarity (M)	Band gap energy (eV)
0.05	6.2
0.10	6.1
0.15	6.0
0.20	5.9

The energy band gap of semiconductors tends to decrease as the molarity is increased. An increased inter atomic spacing decreases the potential seen by the electrons in the material, which in turn reduces the energy band gap.

Functional group analysis of hafnium dioxide nanoparticles: The FTIR spectra of synthesized sample at calcination temperature of 500 °C in different molarities (0.05-0.2 M) of hafnium dioxide are as shown in Fig. 4. The observing at FT-IR spectra it's clear the presence of HfO_2 nanoparticles. The spectra were taken in the range 4000-400 cm^{-1}. While main peaks at 777, 541,433 cm^{-1} due to the formation of Hf-O bonds and in which the range of IR (800-400 cm^{-1}) are photon modes of crystalline hafnium [19]. The absorption band at 1575 cm^{-1} corresponds to the H-O-H bending vibration of adsorbed water. The characteristics absorption bands at 1415 cm^{-1} are assigned to Biden ate carbonate symmetric stretching [20].

Surface morphological analysis: Fig. 5(a-d) gives the SEM micrographs of the surface of hafnium dioxide nanoparticles prepared at different molar concentrations. The surface morphology of the HfO_2 nanoparticles is observed. But, the grain size could not be viewed clearly. From Fig. 5(a,b) one

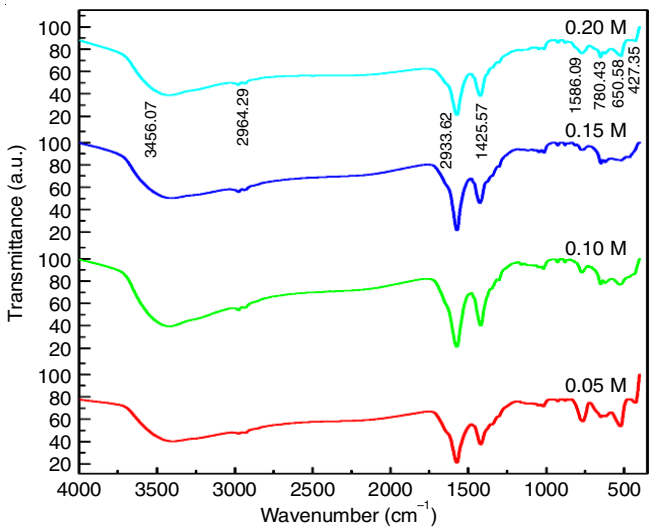

Fig. 4. FTIR spectra of hafnium dioxide (HfO_2) nanoparticles at various molarities

can find that, the microstructure consisted of many plate shaped crystalline particles. The microstructure formed is found to be uniform and compact which are interconnected by grains. These results suggested that the size of the grains is large at low concentration; less than 0.1 M. Further, it is reduced, when the molarity concentration is increased. There by the best uniform surface morphology is identified at 0.2 M. However, the overall observation is that the grain size is decreased and its surface becomes optically flat with increase of concentration. Pure HfO_2 nanoparticles appear like plate in shape of size ~ 1 µm. All these nanoparticles present are in the size range of nm.

Photoluminescence: The photoluminescence spectra of hafnium dioxide nanoparticles was recorded with a view to understand the emission properties of the materials. Photoluminescence emission curves of the molarity (0.05-0.2 M) for hafnium nanoparticals has a broad visible emission band extending from 350 to 600 nm nearly covers the entire visible range showing emission peaks for 0.15 and 0.2 M in 362, 412, 494, 522, 539 and 377 nm [21]. The peaks for 0.05 and 0.1 M are at 361, 410, 493, 519 and 538 nm obtained in the Fig. 6. All peaks range and shift including as shown in Table-3.

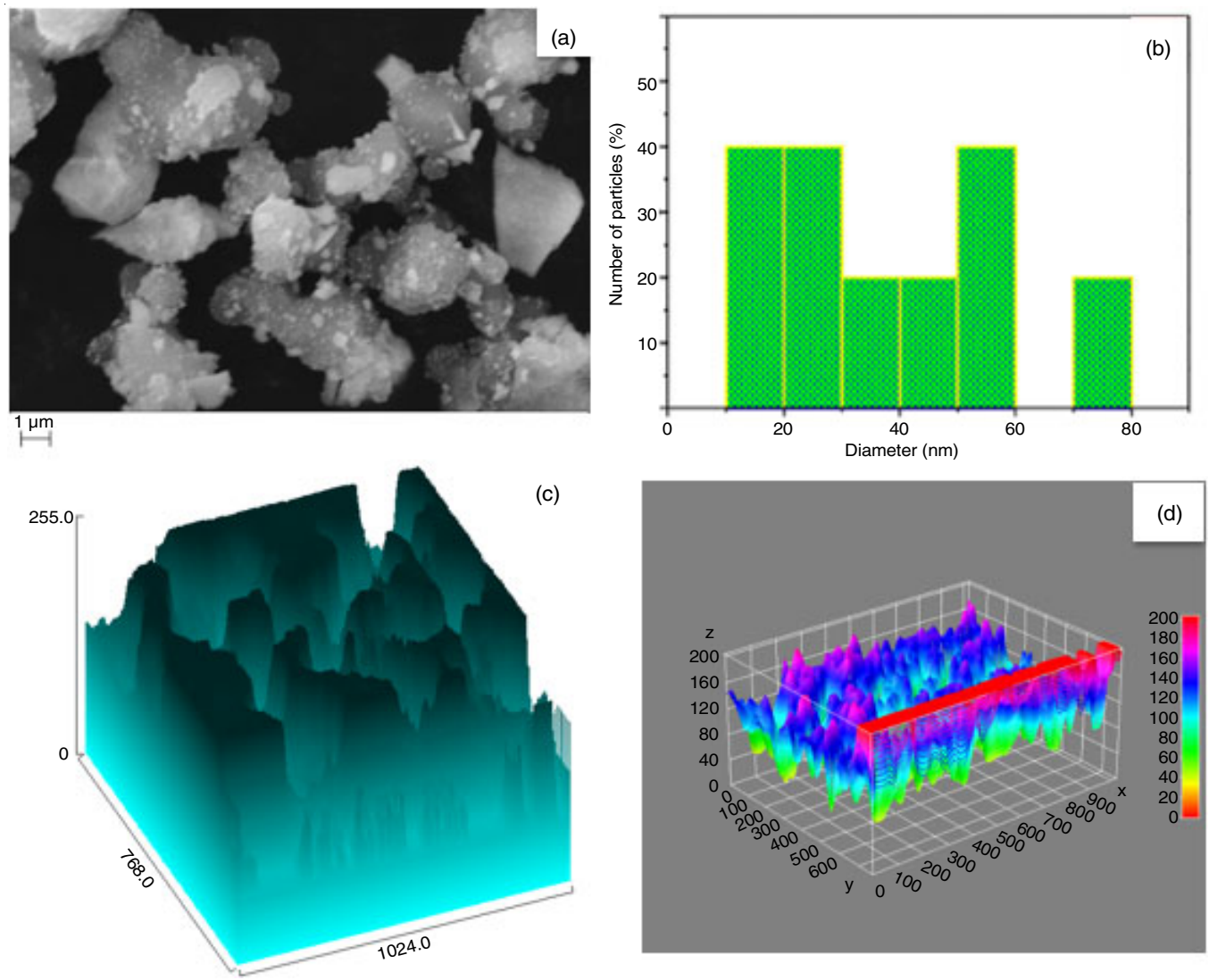

Fig. 5.1. (a) SEM image (b) the size distribution histograms (c) surface occupancy plot (d) surface profile analysis in hafnium oxide (HfO_2) (0.05 M)

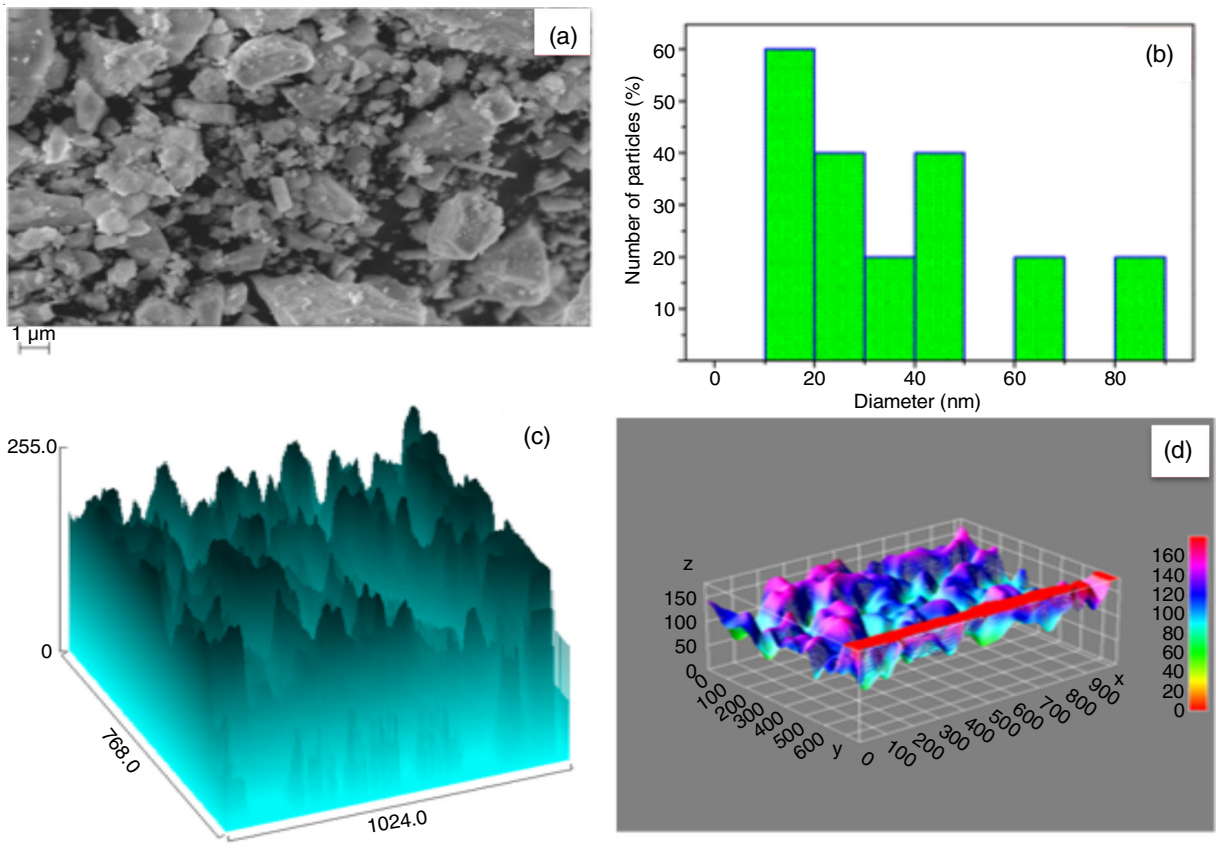

Fig. 5.2. (a) SEM image (b) the size distribution histograms (c) surface occupancy plot (d) surface profile analysis in hafnium oxide (HfO_2) (0.1 M)

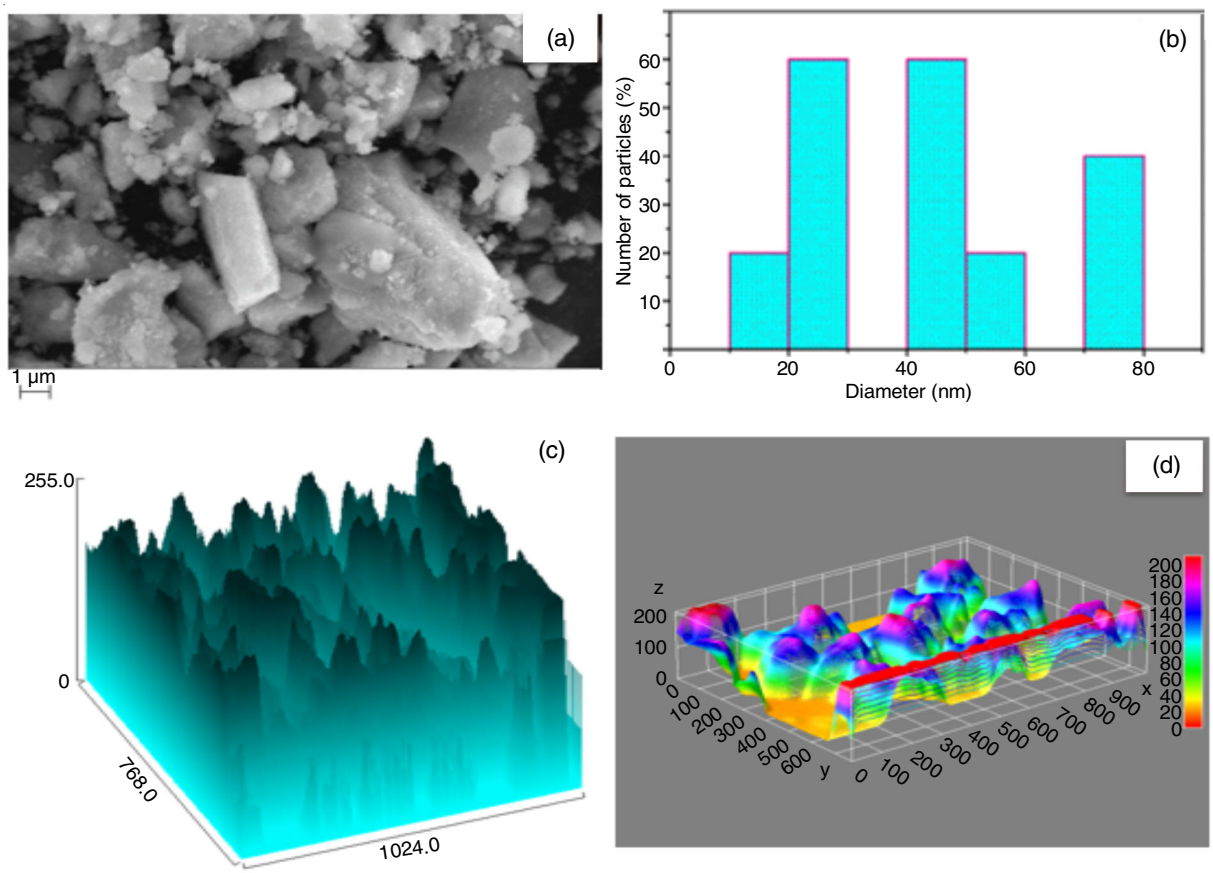

Fig. 5.3. (a) SEM image (b) the size distribution histograms (c) surface occupancy plot (d) surface profile analysis in hafnium oxide (HfO_2) (0.15 M)

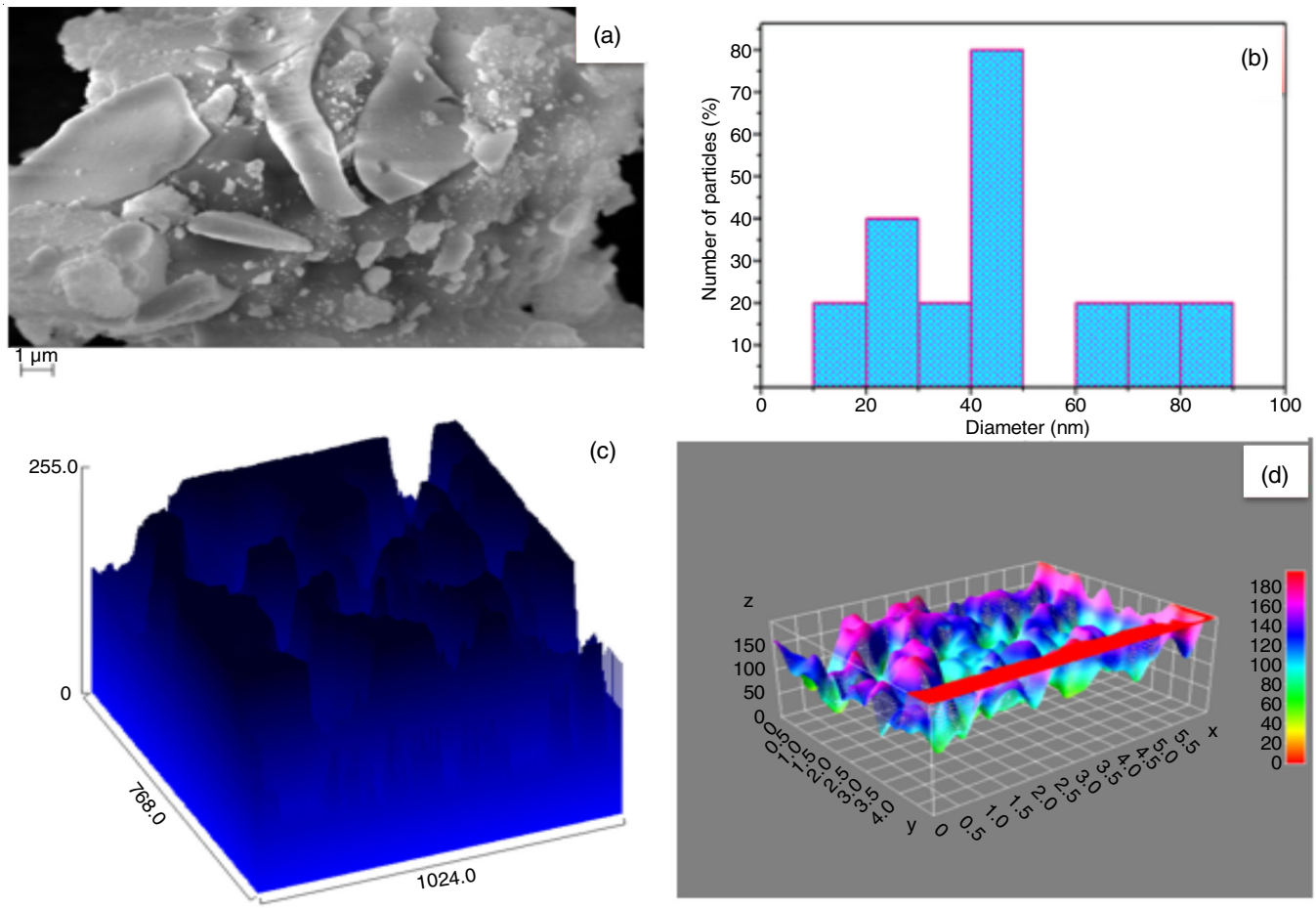

Fig. 5.4. (a) SEM image (b) the size distribution histograms (c) surface occupancy plot (d) surface profile analysis in hafnium oxide (HfO_2) (0.2 M)

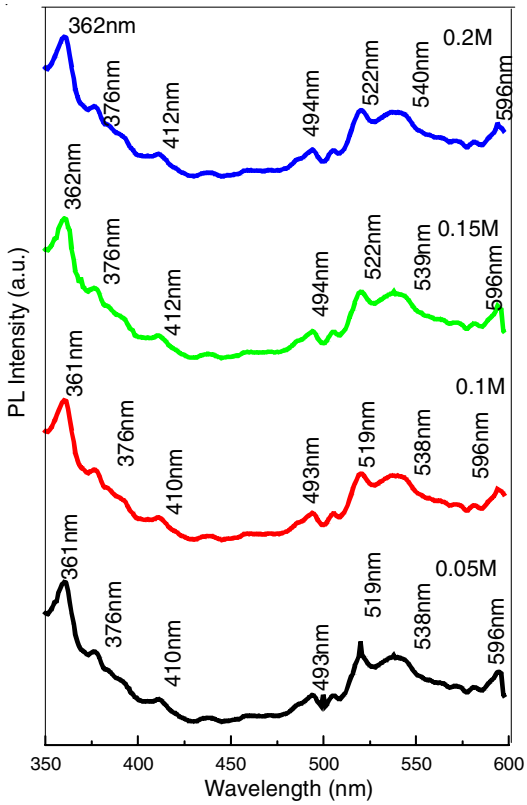

Fig. 6. Photoluminescence spectra of hafnium oxide (HfO_2) nanoparticles at different molarities

TABLE-3
PHOTOLUMINESCENCE SPECTRA OF HAFNIUM OXIDE NANOPARTICLES

Range (nm)	Colour
352-412	Green
413-494	Blue
500-596	Red/Orange

Conclusion

The hafnium oxide nanoparticles were synthesized by a sol-gel method. The study of XRD revealed that the synthesized HfO_2 nanoparticles transformed from cubic structure [JCPDS-53-0560] to monoclinic structure [JCPDS-78-0049] as HfO_2 nanoparticles concentration increase. The optical properties were examined by the UV-visible absorption spectrum. The band gap value was found to be 6.2, 6.1, 6.0 and 5.9 eV. The photoluminescence emission of the sample covers full nearly visible range attributed to the closed level emission which can be considered to be promoted by the morphology and size of the nanoparticles formed. Considering the growth and reproducibility of the HfO_2 nanoparticles visible and emission found in the as formed sample provides better option for LED application.

CONFLICT OF INTEREST

The authors declare that there is no conflict of interests regarding the publication of this article.

REFERENCES

1. M. Mazur, D. Kaczmarek, J. Domaradzki, D. Wojcieszak and A. Poniedzialek, *Coatings*, **6**, 13 (2016); https://doi.org/10.3390/coatings6010013.
2. T.S.N. Sales, F.H.M. Cavalcante, B. Bosch-Santos, L.F.D. Pereira, G.A. Cabrera-Pasca, R.S. Freitas, R.N. Saxena and A.W. Carbonari, *AIP Adv.*, **7**, 056315 (2017); https://doi.org/10.1063/1.4976583.
3. V. Jayaraman, G. Bhavesh, S. Chinnathambi, S. Ganesan and P. Aruna, *Mater. Express*, **4**, 375 (2014); https://doi.org/10.1166/mex.2014.1190.
4. S.A. Eliziário, L.S. Cavalcante, J.C. Sczancoski, P.S. Pizani, J.A. Varela, J.W.M. Espinosa and E. Longo, *Nanoscale Res. Lett.*, **4**, 1371 (2009); https://doi.org/10.1007/s11671-009-9407-6.
5. H. Padma Kumar, S. Vidya, S. Saravana Kumar, C. Vijayakumar, S. Solomon and J.K. Thomas, *J. Asian Ceram. Soc.*, **3**, 64 (2015); https://doi.org/10.1016/j.jascer.2014.10.009.
6. M.F. Al-Kuhaili, S.M.A. Durrani, I.A. Bakhtiari, M.A. Dastageer and M.B. Mekki, *Mater. Chem. Phys.*, **126**, 515 (2011); https://doi.org/10.1016/j.matchemphys.2011.01.036.
7. R.K. Nahar, V. Singh and A. Sharma, *J. Mater. Sci. Mater. Electron.*, **18**, 615 (2007); https://doi.org/10.1007/s10854-006-9111-6.
8. A. Ramadoss, K. Krishnamoorthy and S.J. Kim, *Mater. Lett.*, **75**, 215 (2012); https://doi.org/10.1016/j.matlet.2012.02.034.
9. E.N. Cerón, G.R. Gattorno, J. Guzmán-Mendoza, M. García-Hipólito and C. Falcony, *Open J. Synth. Theory Appl.*, **2**, 73 (2013); https://doi.org/10.4236/ojsta.2013.22009.
10. P. Rauwel, A. Galeckas, M. Salumaa, A. Aasna, F. Ducroquet and E. Rauwel, *IOP Conf. Ser. Mater. Sci. Eng.*, **175**, 012064 (2017); https://doi.org/10.1088/1757-899X/175/1/012064.
11. Y.L. Zhang, Y. Yang, J.H. Zhao, R.Q. Tan, P. Cui and W.J. Song, *J. Sol-Gel Sci. Technol.*, **51**, 198 (2009); https://doi.org/10.1007/s10971-009-1959-5.
12. F.L. Martínez, M. Toledano-Luque, J.J. Gandía, J. Cárabe, W. Bohne, J. Röhrich, E. Strub and I. Mártil, *J. Phys. D Appl. Phys.*, **40**, 5256 (2007); https://doi.org/10.1088/0022-3727/40/17/037.
13. V. Jayaraman, S. Sagadevan and R. Sudhakar, *J. Electron. Mater.*, **46**, 4392 (2017); https://doi.org/10.1007/s11664-017-5432-x.
14. M. Jothibas, S.J. Jeyakumar, C. Manoharan, I.K. Punithavathy, P. Praveen and J.P. Richard, *J. Mater. Sci. Mater. Elem.*, **28**, 1889 (2017); https://doi.org/10.1007/s10854-016-5740-6.
15. V. Porkalai, D.B. Anburaj, B. Sathya, G. Nedunchezhian and R. Meenambika, *J. Mater. Sci. Mater. Elem.*, **28**, 2521 (2017); https://doi.org/10.1007/s10854-016-5826-1.
16. J.P. Richard, I.K. Punithavathy, S.J. Jeyakumar, M. Jothibas and P. Praveen, *J. Mater. Sci. Mater. Electron.*, **28**, 4025 (2017); https://doi.org/10.1007/s10854-016-6016-x.
17. C. Manoharan, M. Jothibas, S. Dhanapandian, G. Kiruthigaa and S.J. Jeyakumar, Role of Titanium Doping on Indium Oxide Thin Films Using Spray Pyrolysis Techniques, International Conference on Advanced Nanomaterials and Emerging Engineering Technologies (ICANMEET) Chennai, India (2013); https://doi.org/10.1109/ICANMEET.2013.6609310.
18. V. Anusha Devi and K.A. Vijayalakshmi, *Int. J. Adv. Sci. Eng.*, **4**, 667 (2018); https://doi.org/10.29294/IJASE.4.3.2018.667-672.
19. A. Ramadoss, K. Krishnamoorthy and S.J. Kim, *Mater. Res. Bull.*, **47**, 2680 (2012); https://doi.org/10.1016/j.materresbull.2012.05.051.
20. N.V. Nguyen, A.V. Davydov, D. Chandler-Horowitz and M.M. Frank, *Appl. Phys. Lett.*, **87**, 192903 (2005); https://doi.org/10.1063/1.2126136.
21. E. Oh, S.-H. Jung, K.-H. Lee, S.-H. Jeong, S.G. Yu and S.J. Rheec, *J. Mater. Lett.*, **62**, 3456 (2008); https://doi.org/10.1016/j.matlet.2008.02.073.